

Effective intravenous delivery of adenovirus armed with TNF α and IL-2 improves anti-PD-1 checkpoint blockade in non-small cell lung cancer

Tatiana V. Kudling^a, James H.A. Clubb^{a,b}, Santeri Pakola^a, Dafne C.A. Quixabeira^{a,b}, Iris A.K. Lähdeniemi^{c,d}, Camilla Heiniö^a, Víctor Arias^a, Riikka Havunen^{a,b}, Víctor Cervera-Carrascon^{a,b}, Joao M. Santos^{a,b}, Eva Sutinen^{d,e,f}, Jari Räsänen^g, Kristian Borenus^{d,g}, Mikko I. Mäyränpää^h, Eero Aaltonenⁱ, Suvi Sorsa^{a,b}, Otto Hemminki^{j,k}, Anna Kanerva^{a,j,l}, Emmy W. Verschuren^{c,d}, Ilkka Ilonen^{d,g}, and Akseli Hemminki^{d,a,b,j}

^aCancer Gene Therapy Group, Translational Immunology Research Program, Faculty of Medicine, University of Helsinki, Helsinki, Finland; ^bTILT Biotherapeutics Ltd, Helsinki, Finland; ^cTranslational Lung Cancer Research Group, Institute for Molecular Medicine Finland (FIMM), HiLife, University of Helsinki, Helsinki, Finland; ^dCAN Digital Precision Cancer Medicine Flagship, Helsinki, Finland; ^eIndividualized Drug Therapy Research Program, Faculty of Medicine, University of Helsinki, Helsinki, Finland; ^fDepartment of Pulmonary Medicine, Heart and Lung Center, Helsinki University Hospital, Helsinki, Finland; ^gGeneral Thoracic and Esophageal Surgery, Heart and Lung Center, Helsinki University Hospital and Faculty of Medicine, University of Helsinki, Helsinki, Finland; ^hPathology, University of Helsinki and Helsinki University Hospital (HUSLAB), Helsinki, Finland; ⁱFaculty of Medicine, Medicum, University of Helsinki, Helsinki, Finland; ^jComprehensive Cancer Center, Helsinki University Hospital (HUS), Helsinki, Finland; ^kDepartment of Urology, Helsinki University Hospital, Helsinki, Finland; ^lDepartment of Gynecology and Obstetrics, Helsinki University Hospital, Helsinki, Finland

ABSTRACT

Lung cancer remains among the most difficult-to-treat malignancies and is the leading cause of cancer-related deaths worldwide. The introduction of targeted therapies and checkpoint inhibitors has improved treatment outcomes; however, most patients with advanced-stage non-small cell lung cancer (NSCLC) eventually fail these therapies. Therefore, there is a major unmet clinical need for checkpoint refractory/resistant NSCLC. Here, we tested the combination of aPD-1 and adenovirus armed with TNF α and IL-2 (Ad5-CMV-mTNF α /mIL-2) in an immunocompetent murine NSCLC model. Moreover, although local delivery has been standard for virotherapy, treatment was administered intravenously to facilitate clinical translation and putative routine use. We showed that treatment of tumor-bearing animals with aPD-1 in combination with intravenously injected armed adenovirus significantly decreased cancer growth, even in the presence of neutralizing antibodies. We observed an increased frequency of cytotoxic tumor-infiltrating lymphocytes, including tumor-specific cells. Combination treatment led to a decreased percentage of immunosuppressive tumor-associated macrophages and an improvement in dendritic cell maturation. Moreover, we observed expansion of the tumor-specific memory T cell compartment in secondary lymphoid organs in the group that received aPD-1 with the virus. However, although the non-replicative Ad5-CMV-mTNF α /mIL-2 virus allows high transgene expression in the murine model, it does not fully reflect the clinical outcome in humans. Thus, we complemented our findings using NSCLC ex vivo models fully permissive for the TNF α and IL-2-armed oncolytic adenovirus TILT-123. Overall, our data demonstrate the ability of systemically administered adenovirus armed with TNF α and IL-2 to potentiate the anti-tumor efficacy of aPD-1 and warrant further investigation in clinical trials.

ARTICLE HISTORY

Received 14 June 2023
Revised 24 July 2023
Accepted 24 July 2023

KEYWORDS



Immunotherapy; checkpoint inhibitors; adenovirus; intravenous administration


Introduction

Despite significant achievements in treatment over the past decade, non-small cell lung cancer (NSCLC) remains an incurable disease. This can be explained by multiple factors affecting cancer progression, including a high mutational burden, immunosuppressive tumor microenvironment (TME), and a high risk of metastasis.^{1–3} The options for patients with inoperable NSCLC are typically kinase inhibitors, chemotherapy, and immunotherapies, and the latter two are frequently used in combination, depending on the PD-L1 status of the tumor.^{4,5} However, over time, patients treated with either approach usually become resistant,^{6,7} thus there is an unmet need for novel efficient therapies for advanced and metastatic

NSCLC in patients failing standard treatments. Oncolytic virotherapy is a promising approach because of its potential to overcome ICIs resistance and improve outcomes in the treatment of advanced NSCLC.⁸

The present study focuses on the integration of immune checkpoint blockade, cytokine therapy, and virotherapy into an effective anticancer tool. Engineered oncolytic viruses (OVs) are attractive therapeutic agents because they combine the selective lysis of tumor cells with host immune system activation. Upon infection, OVs are also able to deliver transgenes to the tumor site, allowing their efficient local expression, and thus concomitant priming of infiltrating immune cells.⁹ Importantly, most OVs have proven satisfactory safety levels in clinical trials when

CONTACT Akseli Hemminki  akseli.hemminki@helsinki.fi  Cancer Gene Therapy Group, Translational Immunology Research Program, Faculty of Medicine, University of Helsinki, Helsinki, Finland

 Supplemental data for this article can be accessed online at <https://doi.org/10.1080/2162402X.2023.2241710>

© 2023 The Author(s). Published with license by Taylor & Francis Group, LLC.

This is an Open Access article distributed under the terms of the Creative Commons Attribution-NonCommercial License (<http://creativecommons.org/licenses/by-nc/4.0/>), which permits unrestricted non-commercial use, distribution, and reproduction in any medium, provided the original work is properly cited. The terms on which this article has been published allow the posting of the Accepted Manuscript in a repository by the author(s) or with their consent.

administered systemically.^{10,11} However, the presence of preexisting neutralizing antibodies, components of the complement system, stromal barriers, and local hypoxic regions, as well as poor vascularization of some types of tumors have been proposed to influence the anti-tumor efficacy of intravenously administered OVs.^{12–15}

We believe that our approach offers several benefits in the context of NSCLC. First, due to high vascularization, NSCLC tumor cells are often accessible to intravenously injected viruses, which in turn can infect and lyse several nodules or metastases simultaneously, making the treatment more effective, feasible, and comfortable for the patients. Second, since the replication of OVs is restricted to malignant cells, the toxicity of the treatment is reduced compared to conventional therapies.¹⁶ Thirdly, OVs are able to convert local TME toward inflammation,¹⁷ thus potentially restoring anti-tumor response to immune checkpoint therapy. Here, we investigated the efficacy of intravenously administered adenovirus encoding TNF α and IL-2 to improve checkpoint blockade in murine lung cancer tumors. Although previously we have shown that combining adenovirus-mediated intratumoral delivery of TNF α and IL-2 with anti-programmed cell death protein 1 (aPD-1) is beneficial in several pre-clinical murine models,^{18–20} in this study we used intravenous route of administration. This approach has a high translational value because local treatment is not always feasible in clinic.

For the *in vivo* experiment, we used adenovirus Ad5-CMV-mTNF α /mIL-2 allowing higher expression of the murine TNF α and IL-2 under CMV promoter, but were unable to replicate and lyse mouse cancer cells. Nevertheless, we previously showed that using of Ad5-CMV-mTNF α /mIL-2 in murine model was able to cause immunological changes and induce tumor growth control in both injected and non-injected tumors even without oncolysis.²¹ To complement *in vivo* results and overcome non-permissiveness issue, we used clinically relevant patient-derived NSCLC *ex vivo* models. In the fully human system, we combined aPD-1 treatment with chimeric oncolytic adenovirus Ad5/3-E2F-d24-hTNF α -IRES-hIL2, a.k.a TILT-123, which is a human adenovirus coding for human transgenes, presently undergoing evaluation in clinical trials (NCT04695327, NCT04217473, NCT05271318, and NCT05222932).

We observed superior tumor growth control *in vivo* when combining aPD-1 with the virus, as well as greater activation of key immune cell subsets, such as NK cells and CD8⁺ T cells, and reduced local immunosuppression, compared to controls. *Ex vivo* model showed similar increase in cytotoxic lymphocytes when aPD-1 was combined with the virus, as well as higher local production of pro-inflammatory cytokines.

In summary, our findings support the rationale for clinical investigation of the combination of ICIs with systemic delivery of oncolytic adenovirus coding for TNF α and IL-2, for example, TILT-123, for treatment of ICI-refractory NSCLC, with such a phase 1 trial being in progress (NCT code pending).

Materials and methods

Cell line and viruses

The Lewis lung carcinoma cell line LL/2 (LLC1) was purchased from ATCC (VA, USA) and cultured in DMEM supplemented with 10% FBS, 2 mM l-glutamine, 100 U/mL penicillin, and 100 mg/mL streptomycin. Cells were incubated at +37°C and 5% CO₂ and passaged *in vitro* three to four times prior to *in vivo* use. Ad5-CMV-mTNF α , Ad5-CMV-mIL-2 (also referred to as Ad5-CMV-mTNF α /mIL-2), and Ad5/3-E2F-d24-hTNF α -IRES-hIL2 adenoviral constructs have been described.^{9,22}

Murine NSCLC experimental models and treatments

LLC1 tumors (1×10^6 cells) were engrafted subcutaneously into 4- to 5-week-old immunocompetent female C57BL/6BrdCrHsd-Tyr mice (Envigo, IN, USA). After the tumors reached 2–3 mm in diameter, the animals were randomized into one of the experimental groups and received four rounds of treatment. Anti-mouse PD-1 antibody (Clone RMPI-14, Bio X Cell, NH, USA) was administered intraperitoneally at 0.1 mg/dose. Equal amounts of Ad5-CMV-mTNF α /mIL-2 viruses, 1×10^9 virus particles (VP) per virus were injected into the tail vein. The mock and aPD-1 monotherapy groups received intravenous injections of phosphate-buffered saline (PBS). Tumors were measured daily using a digital caliper, and tumor volumes were calculated as length \times width²/2. The animals were euthanized on day 10, and their tumors and selected organs were collected for subsequent analysis. None of the animals were euthanized due to the health issues or tumor overprogression.

For *in vivo* depletion, mice were initially injected with 400 μ g of depleting anti-CD8 α (clone 2.43, Bio X Cell, NH, USA), anti-NK1.1 (clone PK136, Bio X Cell, NH, USA), or anti-CD4 antibodies (clone GK1.5, Bio X Cell, NH, USA) 1 day prior to treatment and then 100 μ g every 2 days for the duration of the experiment. The animals received four rounds of treatment and were euthanized on day 10. Blood was collected to verify immune cell depletion. Detailed treatment schedules are described in the respective figures.

Neutralization assay

Neutralizing antibodies (NAb) from complement-inactivated murine serum samples were determined using the Dual-Luciferase[®] Reporter Assay System (Promega, WI, USA), as described previously.²³ The NAb titer was determined to have the lowest dilution of the serum that blocked at least 80% of luciferase activity.

Flow cytometry

Murine tumors were mechanically disrupted into single-cell suspensions, filtered by pressing through 70 μ m filters, and stored at –80°C. For intracellular staining, cells were cultured for 4 h in media containing brefeldin A (BD GolgiPlug[™] containing Brefeldin A, BD, NJ, USA) to inhibit protein transport.

Cell permeabilization and antibody staining were performed using a Cytofix/Cytoperm™ Plus Fixation/Permeabilization Kit (BD, NJ, USA) according to the manufacturer's instructions. Samples were stained after Fc blocking using a Mouse BD Fc block (Clone 2.4G2, BD, NJ, USA). An APC-conjugated tetramer (H-2Kb), loaded with the LLC1 tumor-specific peptide KMYQYARL, was synthesized by Tetramer Shop (Denmark). The complete antibody list is shown in Supplementary table s1.

All samples were acquired in duplicate using a FACS Aria II cell sorter (BD Biosciences), collecting at least 50,000 events per sample. Data analysis was performed using Flowjo software v10 (Flowjo LLC, BD, NJ, USA).

Patient-derived samples processing and establishment of *ex vivo* tumor histocultures

Fresh single-cell tumor digests were prepared from tumors using a previously described protocol.¹⁷ The resulting heterogeneous suspension was used to establish *ex vivo* tumor histocultures by plating 3×10^5 viable cells in triplicate in a 96-well plate and treating them with 100 VP/cell of Ad5/3-E2F-d24-TNF α -IRES-IL-2, 20 mg/ml aPD-1, or their combination. The cells were collected on days 3 and 7 and stored at -140°C until further use. *Ex vivo* sample viability was assessed on days 3, 5, and 7 using 20% of CellTiter 96 AQueous One Solution Proliferation Assay reagent, as described previously.

Ex vivo tumor histocultures viability assay

Tumor cells (3×10^5) were plated in triplicate in a 96-well plate and treated with 100 VP/cell of either Ad5/3-E2F-d24-TNF α -IRES-IL-2, aPD-1, or a combination of both. Cell viability was measured on days 3 and 5 by incubating cells for 2 h with 20% of CellTiter 96 AQueous One Solution Proliferation Assay Reagent (Promega, WI, USA). The absorbance was read at 490 nm using a Hidex Sense plate reader (Hidex, Turku, Finland). The data were normalized to those of the uninfected control group.

Statistical analysis

GraphPad Prism v.8.4.2 (GraphPad Software, MA, USA) was used for statistical analysis and graphical representation of the data. Two-way ANOVA with Tukey' multiple comparison test was performed to evaluate tumor progression, while an unpaired t-test was used to compare treated groups pairwise. Non-parametric Mann-Whitney test was used to compare non-normally distributed data. The results were considered statistically significant when $p < 0.05$.

Results

Treatment with Ad5-CMV-mTNF α /mIL-2 and aPD-1 improves anti-tumor response in mouse LLC1 tumors even in the presence of neutralizing antibodies

To study the anti-tumor benefits of combining aPD-1 with Ad5-CMV-mTNF α /mIL-2, we used mice bearing subcutaneous LLC1 lung carcinoma tumors (Figure 1a). After four rounds of treatment, mice that received the combination had

significantly smaller tumors than the virus alone ($p = 0.0177$), aPD-1 alone ($p < 0.0001$), and mock groups ($p < 0.0001$) (Figure 1b). No significant differences were observed between the mock- and monotherapy-treated groups.

We detected NAb in all analyzed samples obtained from the groups treated with virus only and virus in combination with aPD-1 (Figure 1c). The virus +aPD-1 group showed higher titers of NAb, with a mean value of 1:512, whereas the mean NAb titer in the virus-only group was 1:140. However, no significant differences were observed between the treatment groups.

Intravenous administration leads to adenoviral presence in tumors and a range of normal tissues

We studied the biodistribution of the virus in various tissues (tumors, lungs, spleen, liver, kidneys, and heart) using quantitative real-time PCR. Overall, viral DNA was detected in all the analyzed tissues in both the virus-only and combination groups (Figure 1d). The amount of DNA in the tumors was comparable between the virus-treated groups and reached 10 and 13 E4 copies per pg of gDNA, respectively. Moreover, using viability quantitative real-time PCR,^{24,25} we confirmed the presence of viable viral particles in tumor samples from both virus-treated groups without a statistical difference between them (Figure 1e). Interestingly, the amount of viral DNA in the lungs was higher than in tumors, reaching 286 copies in the virus-only group and 29 copies in the virus+aPD-1 group, suggesting good access to lung micrometastases. Hearts had the lowest amount of viral DNA detected in only two mice in the virus-only group and in one mouse in the combination group.

Overall, the data show that intravenously injected adenoviruses can reach tumors and organs, such as the lungs, through the bloodstream. Moreover, viable viral particles were detected in tumors upon treatment, showing that Ad5-CMV-mTNF α /mIL-2 can be delivered to the tumors by intravenous administration.

Combinatorial treatment with Ad5-CMV-mTNF α /mIL-2 and aPD-1 improves activation and effector functions of tumor-infiltrating immune cells

We evaluated the frequency and diversity of tumor-infiltrating immune cells in the tumor samples collected from the experiment described in Figure 1a. We observed a significantly higher percentage of cytotoxic NK cells expressing granzyme B (GzmB) and interferon gamma (IFN γ) in the combination group than in the virus-only ($p = 0.0214$ and $p = 0.0142$, respectively) and aPD-1 only ($p = 0.0051$ and $p = 0.0004$, respectively) groups. No major differences were observed in the frequency of perforin (Perf) Perf-expressing cells (Figure 2a, upper panel). Additionally, we observed a significantly higher number of functional NK cells expressing the transcription factor T-bet ($p = 0.004$ and $p = 0.0005$, respectively) in the virus+aPD-1 group than in the virus-only and aPD-1 only groups. Moreover, the number of EOMES⁺ NK cells in the virus +aPD-1 group was higher ($p = 0.0083$) than that in the virus-only group (Figure 2a, lower panel).

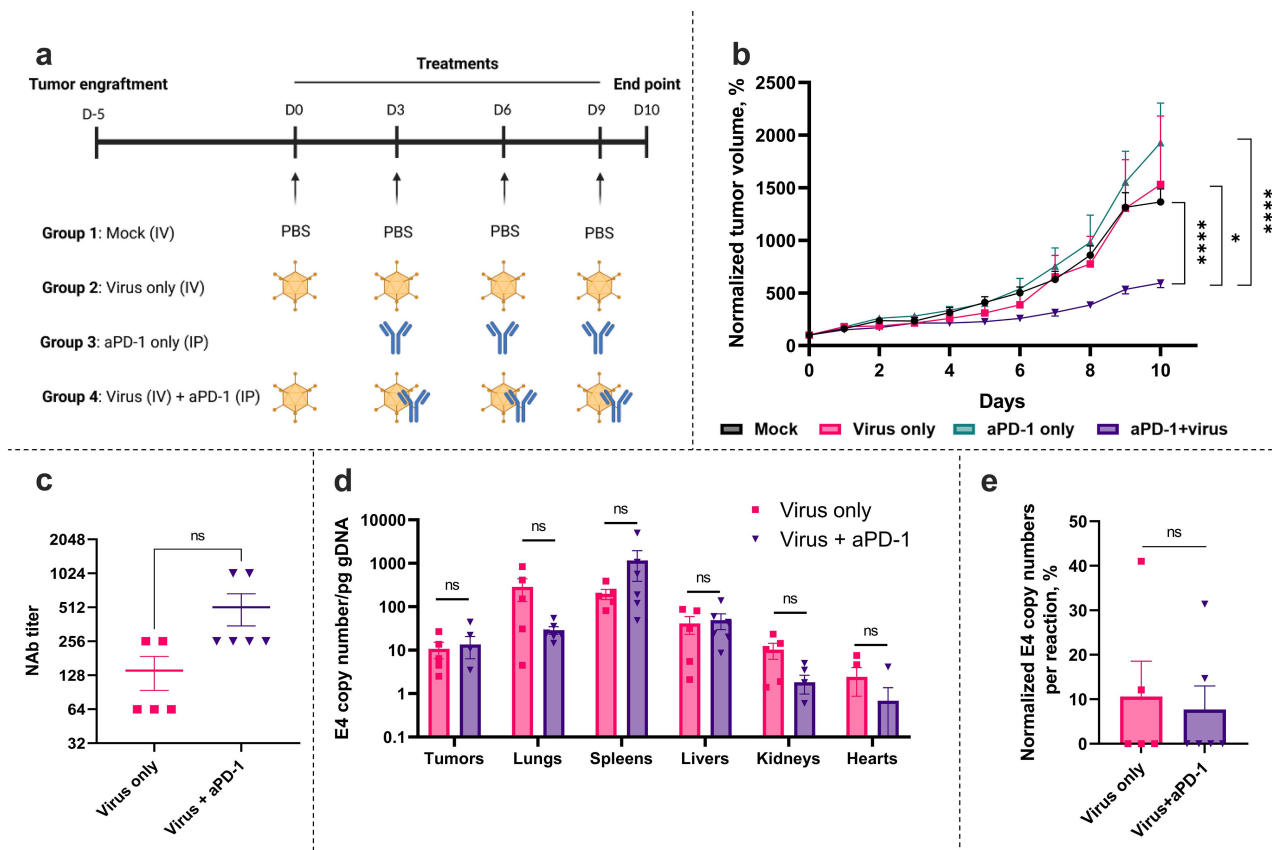


Figure 1. Tumor progression and biodistribution of the virus in syngeneic murine subcutaneous NSCLC model LLC1 after intravenous administration of Ad5-CMV-mTNF α /mIL-2 in combination with aPD-1. **(a)** Experiment design. C57BL/6BrdCrHsd-Tyr mice ($n = 5-6$ per group) were subcutaneously injected with 1×10^6 LLC1 cells into the right flank. After tumors reached 2-3 mm animals were assigned to a group where they were treated with either aPD-1 intraperitoneally (IP), 1×10^9 VPs (non-replicative Ad5-CMV-mTNF α /mIL-2) intravenously (IV), or in combination. Control animals received PBS IV. Treatment frequency as indicated. **(b)** Tumor growth until day 10. Tumor volumes were normalized against day 0. **(c)** Evaluation of the neutralizing antibodies (NAb) titer in serum collected on day 10 by luciferase assay. The NAb titer was determined as the lowest dilution of the serum that blocked at least 80% of luciferase activity. **(d)** Virus distribution evaluation via qPCR using the DNA extracted from snap-frozen tissue fragments. **(e)** Quantification of the viable virions presented in tumor samples by viability PCR. All data is presented as mean \pm SEM. Statistical significance is represented as * $p < 0.05$ and **** $p < 0.0001$.

Similarly, we detected a significantly higher number of cytotoxic GzmB⁺ and Perf⁺CD8⁺ T cells in the combination group than in the virus alone ($p = 0.0025$ and $p = 0.0316$, respectively) and aPD-1 alone ($p = 0.001$ and $p = 0.111$, respectively) (Figure 2b, upper panel). Importantly, we observed a higher number of tumor-specific mRiok1⁺CD8⁺ T cells in the combination group than in the aPD-1 ($p = 0.004$) but not in the virus-only group. Moreover, compared to virus and aPD-1 monotherapies, the number of functional T-bet⁺CD8⁺ T cells ($p = 0.0228$ and $p = 0.0336$, respectively) and EOMES⁺CD8⁺ T cells ($p = 0.039$ and $p = 0.0044$, respectively) in the combination group was significantly higher. The number of activated CD69⁺CD8⁺ T cells was higher in the virus+aPD-1 group than in the aPD-1 only ($p = 0.0029$) but not in the virus-only group (Figure 2b, lower panel).

The analysis of the CD4⁺ T cell population revealed an increase in T-bet⁺ and TNF α ⁺ cells in the virus+aPD-1 group compared to the monotherapies ($p = 0.0259$ and $p = 0.0088$, respectively, for the virus-only group, and $p = 0.0271$ and $p = 0.0324$, respectively, for the aPD-1 only group). No major differences were observed in the percentage of IFN- γ ⁺CD4⁺ T cells (Figure 2c, upper panel). No significant

difference was observed in T regulatory cells (FoxP3⁺CD25⁺CD4⁺ T cells) or cytotoxic EOMES⁺CD4⁺ T cells. The number of exhausted PD-1⁺CD4⁺ T cells was significantly lower in the combination group than in the virus-only only ($p = 0.0241$) but not in aPD-1 only group (Figure 2c, lower panel).

Intratumoral NK cells are primarily involved in anti-tumor efficacy of Ad5-CMV-mTNF α /mIL-2 in combination with aPD1-1 in murine lung LLC1 tumors

To better understand the individual contribution of key immune cell subsets to tumor growth control, we performed a depletion experiment in the same settings as described in Figure 1a (Figure 2d). Blood was collected to confirm that no circulating immune cells were present (Supplementary figure s1). Overall, all mice receiving virus+aPD-1 had significantly smaller tumors than the mock mice (Figure 2e). However, animals from the group pre-treated with anti-NK1.1 antibody had the largest tumors among all depleted groups, although all depleted animals had significantly larger tumors than non-depleted animals ($p < 0.0001$ for anti-NK1.1 depletion, $p = 0.0058$ for

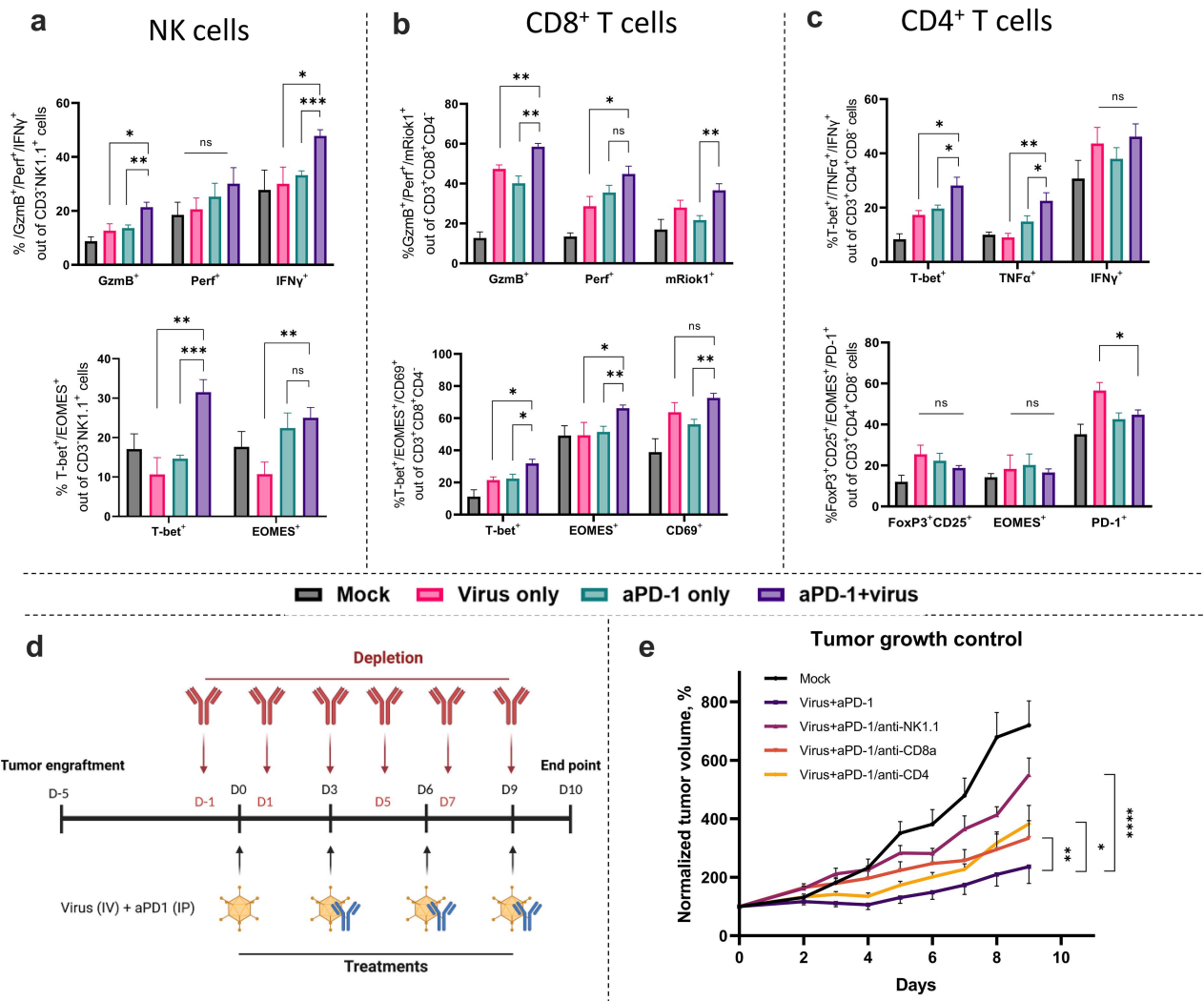


Figure 2. Characterization of tumor-infiltrating immune cells upon intravenous administration of Ad5-CMV-mTNF α /mIL-2 virus in combination with aPD-1. **(a)** Frequency of cytotoxic (GzmB⁺, Perf⁺, IFN γ ⁺) and activated (T-bet⁺, Eomes⁺) NK cells, **(b)** cytotoxic (GzmB⁺, Perf⁺), anti-tumor specific mRiok1⁺ and activated (T-bet⁺, Eomes⁺, CD69⁺) CD8⁺ T cells and **(c)** activated (T-bet⁺, TNF α ⁺, IFN γ ⁺) CD4⁺ T cells as well as immunosuppressive Tregs (CD25⁺FoxP3⁺) and (EOMES⁺, PD-1⁺) CD4⁺ T cells. All flow cytometry experiments were run in technical duplicates, and resulting data is presented as mean \pm SEM. **(d)** Experiment design. C57BL/6BrdCrHsd-Tyr mice ($n = 6$ per group) were subcutaneously injected with LLC1 cells into the right flank. After tumors reached 2-3 mm animals were assigned to a group where they received depleting anti-mouse CD8a, anti-mouse NK1.1 or anti-mouse CD4 antibodies intraperitoneally. Next day animals were treated with combination Apd-1 intraperitoneally (IP) and 1×10^9 VPs (non-replicative Ad5-CMV-mTNF α /mIL-2) intravenously (IV). Control animals received PBS IV. Treatment and depletion frequency as indicated. **(e)** Tumor growth until day 9. Tumor volumes were normalized against day 0. All data is presented as mean \pm SEM. Statistical significance is represented as * $p < 0.05$, ** $p < 0.01$, *** $p < 0.001$, and **** $p < 0.0001$.

anti-CD8a depletion, and $p = 0.0456$ for anti-CD4 depletion) (Figure 2e). Moreover, no significant difference was observed between CD8a-depleted and CD4-depleted animals.

These data suggest that a range of immune cells, including NK cells and CD4⁺ and CD8⁺ T cells, are involved in the anti-tumor response upon combinatorial treatment, with NK cells showing the most prominent impact.

Treatment with Ad5-CMV-mTNF α /mIL-2 favors proinflammatory M1 tumor-associated macrophages and improves dendritic cells maturation and migration

We evaluated the status of tumor-associated myeloid cells – macrophages (TAMs) and dendritic cells (DCs) in samples

obtained from the experiments described in Figure 1a. First, by analyzing the activation of macrophages, we found a higher number of classically activated M1 type macrophages ($p = 0.0137$) and a lower percentage of alternatively activated M2 type macrophages ($p = 0.0361$) in the group treated with virus+aPD-1, compared to aPD-1 alone but not virus alone (Figure 3a). Accordingly, the ratio of M1/M2 macrophages was significantly higher in the virus+aPD-1 group ($p = 0.0334$) compared than in aPD-1 only (Figure 3b). aPD-1 monotherapy did not affect macrophage status. Next, we determined the intratumoral concentration of GM-CSF, a cytokine that promotes immunosuppressive activity of myeloid cells in some pre-clinical models, including lung cancer.^{26,27} We observed a significant decrease in GM-CSF expression in the virus+aPD-1 group

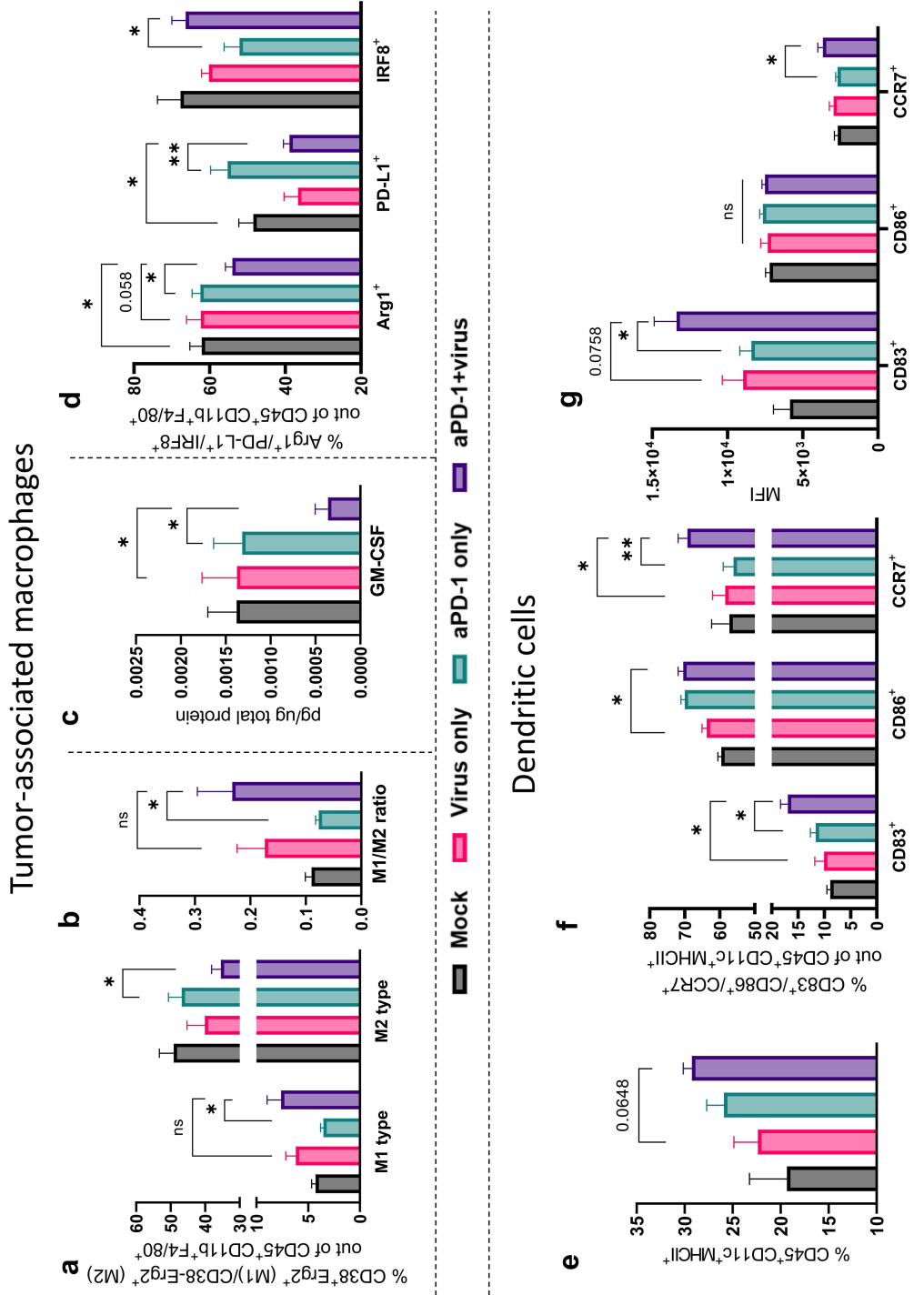


Figure 3. Characterization of tumor-infiltrating myeloid immune cells upon intravenous administration of the virus in combination with Apd-1 following the experimental set-up described in Figure 1a. **(a)** Frequency of M1 and M2 type macrophages and **(b)** their ratio. **(c)** Concentration of GM-CSF in tumor samples measured by cytometric bead array (CBA). **(d)** Frequency of tumor-associated macrophages expressing suppression markers Arg1, PD-L1 and transcriptional factor IRF8. **(e)** Percentage of dendritic cells (DCs) in tumor samples. **(f)** Frequency of dendritic cells expressing maturation and migration markers CD83, CD86 and CCR7 and **(g)** their abundance represented as mean fluorescent intensity (MFI). All flow cytometry experiments were run in technical duplicates and the resulting data are presented as mean±SEM. Statistical significance is represented as **p* < 0.05 and ***p* < 0.01.

compared to that in the virus ($p=0.0272$) and aPD-1 ($p=0.0208$) monotherapy groups (Figure 3c). Moreover, we evaluated the number of macrophages expressing the transcriptional regulators of suppressive markers arginase 1 (Arg1), PD-L1, and IRF8 for myeloid commitment and function. We found a decrease in Arg1⁺ and PD-L1⁺ macrophages in the combination group compared with that in the aPD-1 monotherapy ($p=0.0289$ and $p=0.0062$, respectively) but not virus monotherapy. The number of IRF8⁺ cells was also significantly higher ($p=0.0260$) in the group treated with virus+aPD-1 compared with aPD-1 alone (Figure 3D). The number of infiltrating dendritic cells was higher in the tumors treated with the combination than in the mock and monotherapy groups, although this difference was not significant (Figure 3E). Moreover, we observed a higher percentage of mature DCs expressing CD83 in the virus+aPD-1 group than in the virus ($p=$

0.0151) and aPD-1 only ($p=0.0117$) groups, as well as CD86, but only compared to virus monotherapy ($p=0.0126$). Additionally, the number of migrating CCR7⁺ DCs was higher in the group treated with combination therapy in the virus ($p=0.038$) and aPD-1 alone ($p=0.0077$) groups (Figure 3F). The abundance of CD83 and CCR7 receptors on the surface of DCs was also higher in the virus+aPD-1 group than in the aPD-1 monotherapy ($p=0.0491$ and $p=0.0216$, respectively), whereas the expression of CD86 was similar across the groups.

Treatment with Ad5-CMV-mTNF α /mIL-2 combined with aPD-1 improves immune memory formation

To evaluate memory immune cell compartments, we profiled the peripheral lymphoid organs (inguinal lymph nodes and spleens), which revealed a significant increase in the CD4⁺

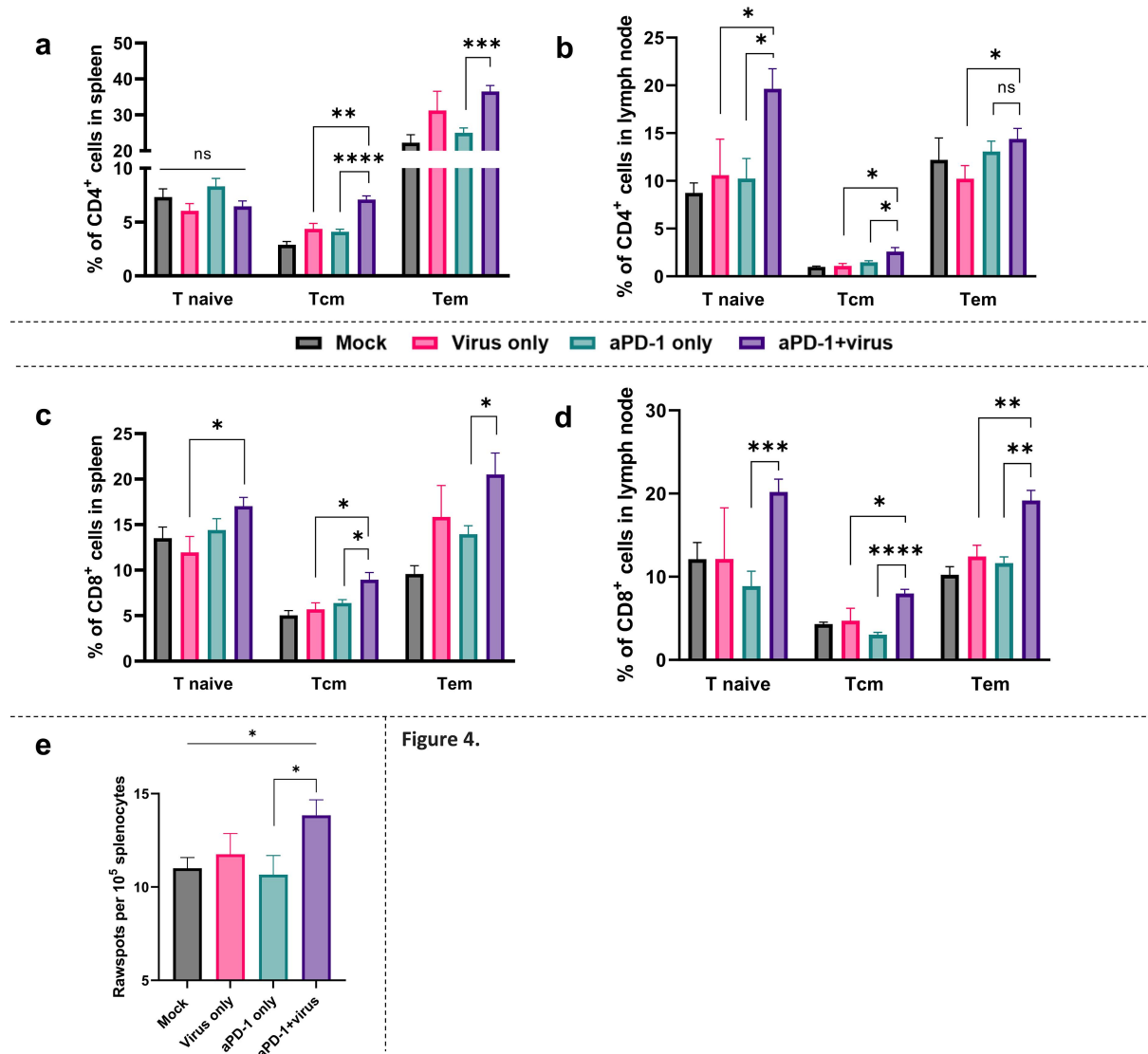


Figure 4. Combining aPD-1 with Ad5-CMV-mTNF α /mIL-2 improves the formation of immune memory in the secondary lymphoid organs. **(a)** Flow cytometric analysis of CD4⁺ T cells in splenic and **(b)** lymph node memory compartment (naïve, effector memory [T_{EM}], central memory [T_{CM}]) from mice bearing LLC tumors as measured by \pm expression of CD44 and CD62L. **(c)** Flow cytometric analysis of CD8⁺ T cells in splenic and **(d)** lymph node memory compartment measured in the same manner. All flow cytometry experiments were run in technical duplicates. **(e)** ELISpot quantification of reactive splenocytes to LLC cells. The resulting data is presented as mean \pm SEM. Statistical significance is represented as * $p < 0.05$, ** $p < 0.01$, *** $p < 0.001$ and **** $p < 0.0001$.

and CD8⁺ effector and central memory compartments when using combination treatment compared to monotherapies. In particular, the percentage of central memory (Tcm) CD44⁺CD62L⁺CD4⁺ T cells was significantly higher in the virus+aPD-1 group than in the virus and aPD-1 only groups ($p = 0.0017$ and $p < 0.0001$, respectively) in the spleen (Figure 4a), as well as in the lymph nodes ($p = 0.0249$ and $p = 0.0277$, respectively) (Figure 4b). Moreover, splenic effector memory (Tem) CD44⁺CD62L⁻CD4⁺ T cells showed an increase in the combination group compared to aPD-1 ($p = 0.0003$) (Figure 4a), while more CD4⁺ Tem cells were detected in the lymph nodes of the animals treated with the combination than in the virus-only only ($p = 0.0472$). In addition, lymph nodes from combination-treated mice showed higher numbers of naïve CD4⁺ T cells compared to virus-treated ($p = 0.05$) and aPD-1-treated ($p = 0.0104$) animals (Figure 4b).

We further found that CD44⁺CD62L⁺CD8⁺ Tcm cells showed a significant increase in both spleens (Figure 4c) and lymph nodes (Figure 4d) of animals treated with the combination compared to those treated with the virus ($p = 0.0197$ and $p = 0.0408$, respectively) and aPD-1 only ($p = 0.0137$ and $p < 0.0001$, respectively). The number of CD44⁺CD62L⁻CD8⁺ Tem cells in the virus+aPD-1 group was higher than that in the aPD-1 only both in the spleens ($p = 0.0269$) (Figure 4c) and lymph nodes ($p = 0.0004$), while it was also higher ($p = 0.0071$) than that in the latter (Figure 4d).

Additionally, we observed a specific anti-tumor response generated in LLC1 tumors via ELISpot. The raw spot count was statistically higher in the virus+aPD-1 group than in the aPD-1 group ($p = 0.0372$) and mock ($p = 0.0374$) groups. No significant difference was observed between the virus-treated and combination groups (Figure 4e).

We conclude that treatment with Ad5-CMV-mTNF α /mIL-2 and aPD-1 expands the population of memory immune cells in secondary lymphoid organs and induces tumor-specific immune memory.

Treatment with Ad5/3-E2F-d24-hTNF α -IRES-hIL-2 in combination with aPD-1 creates an immunostimulatory TME

To further investigate immunological changes in the TME upon treatment, we used a highly clinically relevant human *ex vivo* tumor model treated with a 5/3 chimeric adenovirus encoding human TNF α and IL-2 - Ad5/3-E2F-d24-hTNF α -IRES-hIL-2 (also known as TILT-123). We studied a variety of human lung cancer samples comprising different NSCLC histological subtypes and stages, PD-L1%, and previous treatments (Supplementary table s2). Due to the small size of patient-derived tumor samples, available samples were split for cytotoxicity, cytokine, and flow cytometric analyses. Cell viability by MTS showed effective cell killing following treatment with the virus alone or in combination with aPD-1 was used: the viability reduced to 40–50% by day 7 in both HUSLU1 and HUSLU2 samples (Figure 5a).

To evaluate the expression levels of key pro- and anti-inflammatory cytokines, we measured the concentration of immune signaling molecules in the cell culture supernatants 3 days after infection with HUSLU3, HUSLU6,

HUSLU7, HUSLU8, and HUSLU9. Overall, aPD-1 treatment did not lead to any significant upregulation of cytokine expression, while addition of the virus led to higher expression of proinflammatory IL-2 ($p = 0.0079$), TNF α ($p = 0.0286$), IL-12p40 ($p = 0.0476$), IL-12p70 ($p = 0.0079$), IL-9 ($p = 0.0159$), IL-15 ($p = 0.0476$), MIF ($p = 0.0079$), and CXCL10 ($p = 0.05$), among others (Figure 5b and Supplementary figure s2) compared to aPD-1 monotherapy. Moreover, the combination of virus and aPD-1 led to higher expression of IL-9 ($p = 0.0476$), MIF ($p = 0.0317$), and CXCL10 compared to virus only. The expression of anti-inflammatory IL-4, IL-10, IL-13 and MIF was also higher in the virus+aPD-1 group than in the aPD-1 alone group but not in the virus alone group. No changes were observed for the proinflammatory cytokines IFN γ , TRAIL, IL-6, IL-7, IL-16, anti-inflammatory cytokine IL-1ra, chemokines CCL2, CCL7, CCL11, CCL27, and CXCL1, and growth factors VEGF, SCF, MSCF, and HGF (Supplementary figure s2).

Treatment with Ad5/3-E2F-d24-hTNF α -IRES-hIL2 in combination with aPD-1 activates tumor-infiltrating lymphocytes in NSCLC *ex vivo* tumor histocultures

We determined the activated and cytotoxic tumor-infiltrating lymphocytes in *ex vivo* tumor histocultures HUSLU9, HUSLU10, and HUSLU12 treated with TILT-123, aPD-1, or their combination. Similar to the cytokine profiling, aPD-1 monotherapy did not cause significant changes in the studied immune cell populations. However, when combined with TILT-123, the numbers of GzmB⁺ and Perf⁺CD8⁺ T cells were significantly higher ($p < 0.05$) in all samples (Figure 6a). Moreover, we observed an additive effect of aPD-1 and the virus when evaluating T-bet and EOMES for samples HUSLU9 and HUSLU12, showing higher numbers of T-bet⁺CD8⁺ ($p < 0.01$) and EOMES⁺CD8⁺ T cells ($p < 0.05$) compared to monotherapies (Figure 6b). Lastly, the number of activated CD137⁺CD8⁺ T cells and CD69⁺CD8⁺ T cells was significantly higher in the combination group than in the aPD-1 ($p < 0.05$ and $p < 0.01$, respectively). In HUSLU12, the number of CD137⁺CD8⁺ T cells in the combination group was also higher than in the virus-only group ($p = 0.0288$) (Figure 6c). Overall, despite the variations between the tumor histocultures, treatment with virus +aPD-1 significantly increased the number of activated cytotoxic CD8⁺ T cells (Supplementary figure s3A).

We found a significantly higher number of IFN γ ⁺CD4⁺ and TNF α ⁺CD4⁺ T cells in all samples treated with virus +aPD-1 than in those treated with aPD-1 alone ($p < 0.01$). The number of IFN γ ⁺CD4⁺ T cells in HUSLU12 was also significantly higher than that in the virus alone ($p < 0.05$), while for other samples, a positive trend was observed (Figure 6d). Moreover, we detected a higher percentage of T-bet⁺CD4⁺ T cells in all samples treated with the combination compared to aPD-1 ($p < 0.05$) and virus alone in samples HUSLU9 ($p < 0.05$) and HUSLU12 ($p < 0.05$). Activated CD4⁺ T cells expressing CD137 and CD69 were also more abundant in the combination group in all samples ($p < 0.05$) than in the aPD-1 only. A similar trend was observed with

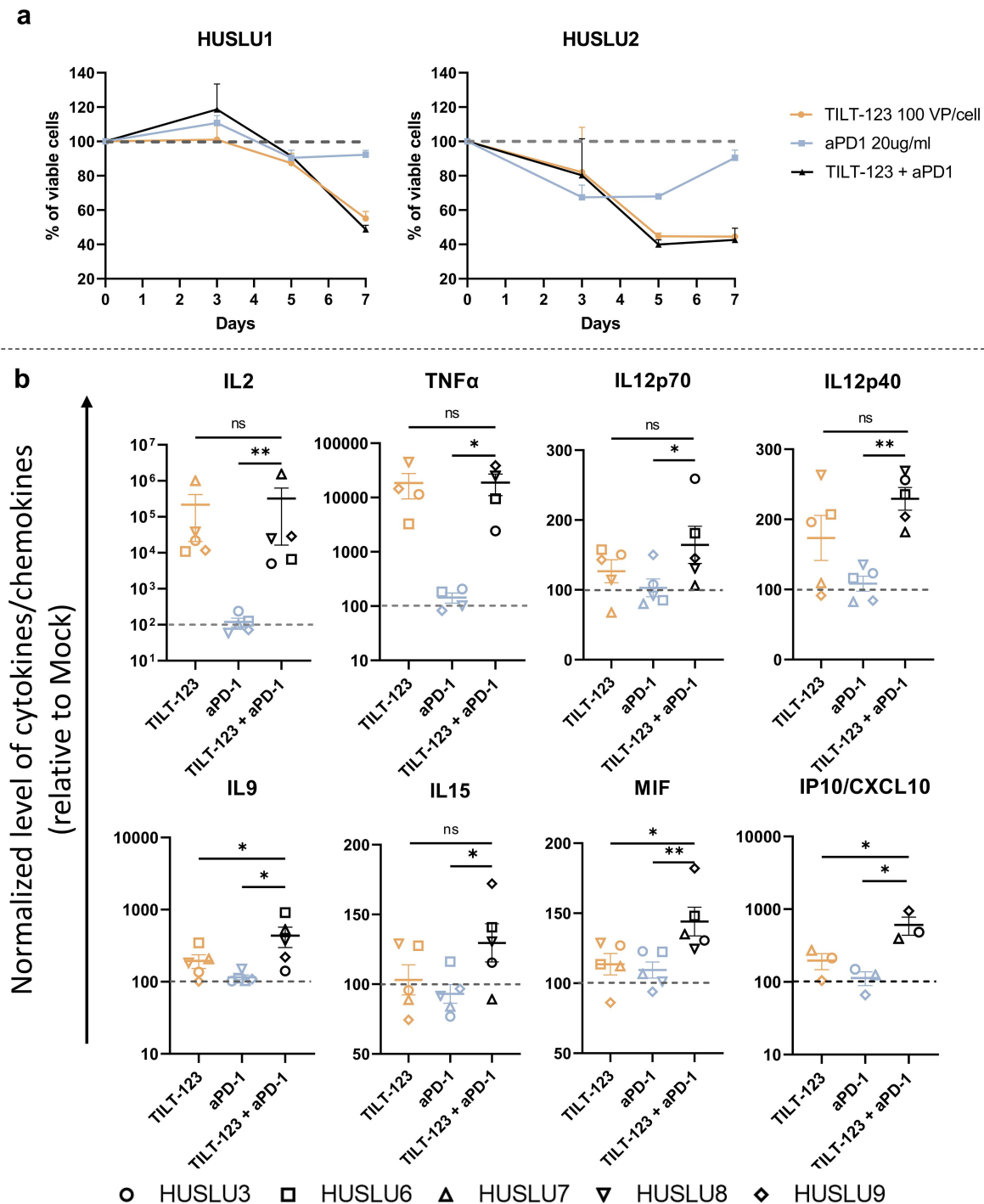


Figure 5. Evaluation of cytokine expression in tumor microenvironment of NSCLC *ex vivo* tumor histocultures. Patient tumor samples were treated with TILT-123 (100 VP/ml), aPD-1 (20 mg/mL) or a combination of TILT-123 and checkpoint inhibitor. Data was normalized to uninfected mock control. **(a)** Viability of tumor digests HUSLU1 and HUSLU2 from NSCLC measured by incubating cells for 2 h with 20% of CellTiter 96 Aqueous One Solution Proliferation Assay reagent (Promega, Wisconsin, USA). Absorbance was read at 490 nm using a Hidex Sense plate reader (Hidex, Turku, Finland). Data was normalized to the uninfected mock control group. Experiments were performed in triplicates. **(b)** Selected cytokines and chemokines changes in tumor microenvironment upon treatments. Resulting data is presented as mean \pm SEM. Statistical significance is represented as * $p < 0.05$ and ** $p < 0.01$.

virus monotherapy compared with aPD-1 monotherapy, although the difference was not statistically significant (Figure 6e). Overall, the combination treatment induced better activation and production of proinflammatory cytokines by CD4⁺ T cells in all NSCLC tumor samples (Supplementary figure s3B).

A similar trend was observed for infiltrating NK cells. We detected a statistically higher frequency of cytotoxic GzmB⁺ and Perf⁺ NK cells in all samples treated with virus+aPD-1 ($p < 0.05$), but only when compared with aPD-1 monotherapy (Figure 6f and Supplementary figure s3C).

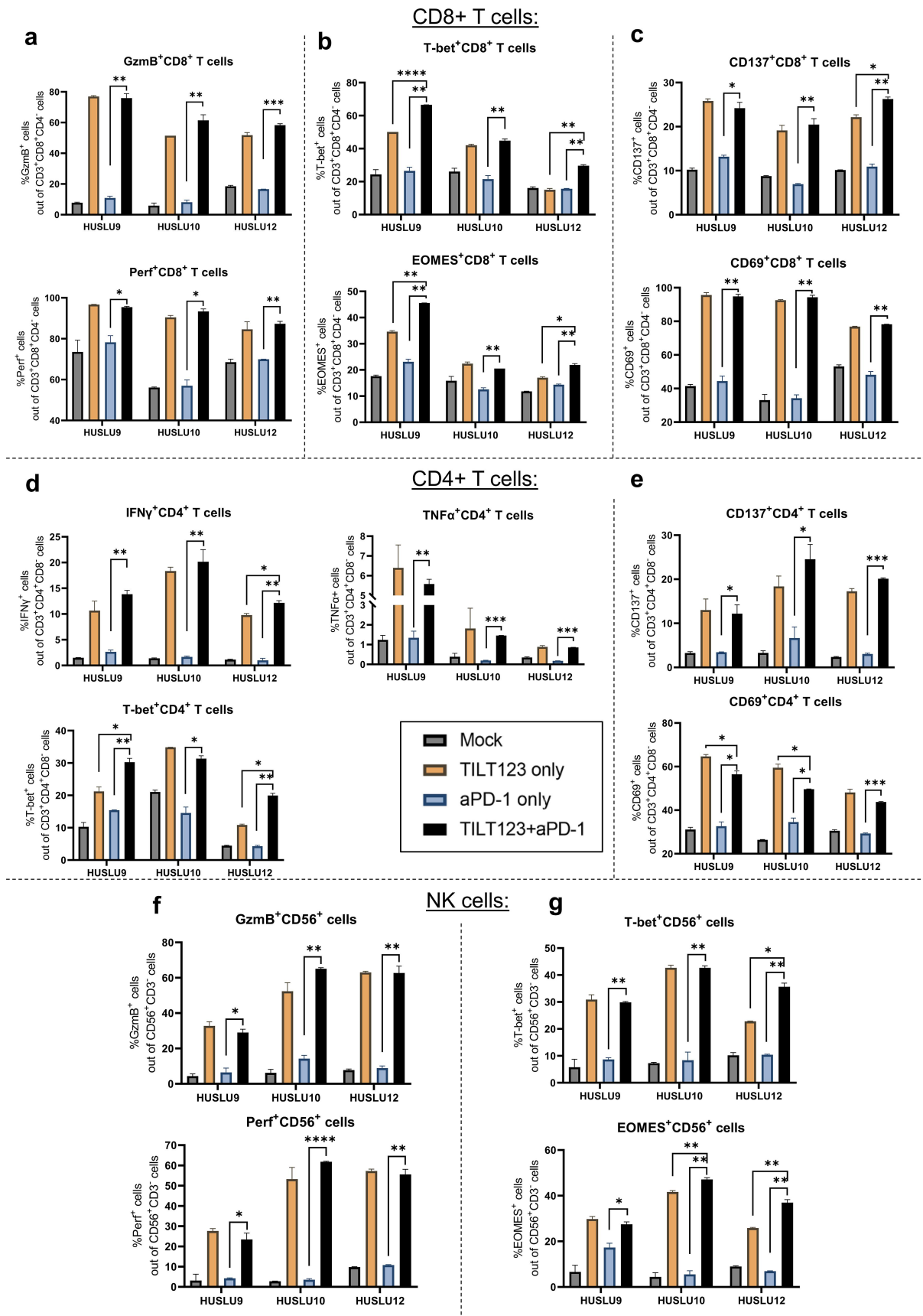


Figure 6. Evaluation of immune cell populations in tumor microenvironment of NSCLC *ex vivo* tumor histocultures: HUSLU9, HUSLU10 and HUSLU12. Patient tumor samples were treated with TILT-123 (100 VP/ml), aPD-1 (20 mg/mL) or a combination of TILT-123 and checkpoint inhibitor. Uninfected cells were used as a mock control. **(a)** Frequency of cytotoxic GzmB⁺ and Perfr⁺ CD8⁺ T cells; **(b)** T-bet⁺ and EOMES⁺ CD8⁺ T cells; **(c)** activated CD69⁺ and CD137⁺ CD8⁺ T cells. **(d)** Frequency of IFN γ ⁺, TNF α ⁺ and T-bet⁺ CD4⁺ T cells; **(e)** activated CD69⁺ and CD137⁺ CD4⁺ T cells. **(f)** Frequency of cytotoxic GzmB⁺ and Perfr⁺ NK cells; **(g)** T-bet⁺ and EOMES⁺ NK cells. All experiments were performed in duplicates, and resulting data is presented as mean \pm SEM. Statistical significance is represented as * $p < 0.05$, ** $p < 0.01$, *** $p < 0.001$ and **** $p < 0.0001$.

Discussion

In this study, we evaluated the ability of intravenously administered adenovirus armed with TNF α and IL-2 to potentiate immune checkpoint blockade in lung cancer. These cytokines were selected empirically based on their ability to activate T cells,²⁸ which is important for the overall efficacy of our approach in the context of checkpoint blockade since it exerts the effects through T cells.²⁹ Thus, for the murine *in vivo* experiment, we used adenovirus Ad5-CMV-mTNF α /mIL-2 allowing higher expression and activity of murine version of transgenes under CMV promoter. Moreover, murine NSCLC model LLC1 which was used in the present study is reported to be refractory to ICIs treatment,^{30,31} which makes our data more valuable for the translation perspective.

Non-permissive murine models have their limitations and do not fully represent the clinical situation in humans. However, the Syrian hamster semi-permissive model,⁹ which we have used often in our preclinical studies of oncolytic adenoviruses, was not feasible due to the lack of hamster lung cancer models and the difficulty of intravenous injections in animals lacking the tail vein. A humanized murine model would allow adenovirus replication, but immunological studies would be limited due to an incomplete hybrid immune system. Thus, to complement *in vivo* results and overcome the non-permissiveness issue, we used clinically relevant patient-derived NSCLC *ex vivo* models. We combined aPD-1 treatment with chimeric oncolytic adenovirus Ad5/3-E2F-d24-hTNF α -IRES-hIL2 (TILT-123) which allows high-level cytokine production in human cells due to the productive virus replication.

In vivo data showed improved anti-tumor efficacy of aPD-1 when combined with the adenovirus armed with TNF α and IL-2, whereas monotherapy did not alter tumor growth. Interestingly, the presence of NAb in animals treated with the combination did not compromise the anti-tumor response. Moreover, the NAb titer in this group was higher than that in the virus alone group, although no statistical significance was observed. This may be because ICIs therapy in combination with viruses may cause significant elevation in B plasma cells and IgG signatures in several pre-clinical models.^{19,32,33}

A virus distribution study confirmed that systemically injected virus can reach distant tumors and several organs, including the lungs, and there was no significant difference if aPD-1 was co-administered. Importantly, the amount of viral DNA detected in the lungs was comparable to that detected in tumors, which confirms the rationale for using OVVs to treat lung cancers, including micrometastases. A significant amount of viral DNA was detected in the liver, most likely because Kupffer cells in the liver sequester adenoviruses from the bloodstream.³⁴ Moreover, our previous data showed that one of the mechanisms adenoviruses can use to avoid neutralizing antibodies and reach distant tumors is binding to erythrocytes and lymphocytes,³⁵ thus we observed viral DNA in spleens, kidneys, and hearts. Importantly, we observed viable virions in both groups treated with Ad5-CMV-mTNF α /mIL-2 but not in every sample. One aspect influencing this is that the method has limitations, allowing

detection of only viruses that did not enter the cell and therefore retain a fully intact capsid. Thus, sample collection timing is crucial for reliable results and may underestimate the amount of viable virus reaching the tumor cells.

Analysis of tumor-infiltrating immune cell populations showed a significantly higher percentage of cytotoxic NK cells expressing IFN γ and GzmB in animals treated with virus+aPD-1, which was further confirmed in *ex vivo* patient-derived model. These findings are important in the context of lung tumors typically infiltrated with low-cytotoxic NK cells possessing impaired expression of granzyme B, thus leading to reduced anti-tumor efficacy and cancer progression.³⁶

Indeed, the results of the depletion experiment support the importance of NK cells for better control of tumor growth. Local attenuation of NK cell killing potency is explained by the specific stage of NK differentiation and the immunosuppressive microenvironment.³⁷ Hence, we studied the expression of T-bet and EOMES – transcriptional factors regulating immune cell development, maturation, and effector functions.³⁸ Our data show that the combinatorial treatment led to a higher percentage of intratumoral functional T-bet⁺ and EOMES⁺ NK cells, which are crucial for anti-tumor response. Indeed, previous studies have shown that downregulation of T-bet and EOMES in adoptively transferred NK cells reduced effective control of tumor growth.³⁹ A higher percentage of T-bet⁺ and EOMES⁺ NK cells in the virus+aPD-1 group can be explained by the local production of several cytokines, including IL-12 and IL-15, which are known to induce T-bet and EOMES expression through JAK/STAT or PI3K-AKT-mTORC1 signaling pathways.⁴⁰ Additionally, restored NK cell cytotoxicity can be influenced by the direct action of aPD-1. It was previously shown that PD-1⁺ NK cells demonstrate a weaker ability to secrete IFN γ , GzmB, and perforin,⁴¹ and blocking this receptor led to the improved release of cytotoxic molecules.⁴² Overall, these aspects may contribute to superior tumor growth control in animals treated with aPD-1 in combination with an oncolytic adenovirus armed with TNF α and IL-2.

The immunosuppressive microenvironment is another aspect of NK cell dysfunction. Myeloid-derived suppressive cells, M2 macrophages, and T regulatory cells contribute to immune exhaustion via the expression of inhibitory ligands, suppressive cytokines, and tumor-promoting factors.⁴³ Moreover, exclusion of functional mature dendritic cells (DCs) from NSCLC tumors and downregulation of DCs effector molecules, such as CD40, CD80, CD86, MHCII, and IL-12, which affect NK cell activity, migration, and survival.^{44,45} We analyzed intratumoral myeloid cells and found a higher proportion of proinflammatory M1 type macrophages and matured DCs as well as increased expression of several DCs and macrophage-secreted cytokines, boosting IFN γ production by NK cells, IL-15, IL-18, and CXCL10, in groups that received viruses. We also observed a higher percentage of macrophages expressing IRF8, which is important for myeloid cell lineage differentiation, and loss of this transcriptional factor leads to accumulation of MDCs.⁴⁶

Analysis of tumor-associated macrophages showed a lower number of cells expressing the M2 macrophage-related

proteins arginase 1 (Arg1) and PD-L1 in both groups treated with the virus. Interestingly, aPD-1 alone did not show any changes in PD-L1⁺ macrophages compared to untreated animals. This finding is in line with previously published data stating that the resistance of the LLC1 cell line to checkpoint blockade correlates with the presence of PD-L1-expressing macrophages.⁴⁷ Thus, combining aPD-1 treatment with the virus is potentially able to break this resistance.

Similar to the NK cells, we found an increased number of cytotoxic CD8⁺ T cells expressing Gzmb, T-bet, and EOMES in the virus+aPD-1 group. However, an important question is whether the treatment can stimulate specific anti-tumor responses. Using the recently discovered⁴⁸ LLC1-specific neoantigen mRiok1, we confirmed a higher number of antigen-specific CD8⁺ T cells in tumors from the combination group. Moreover, we detected an expansion of the memory T cell compartment in the lymph nodes and spleens and an increased number of tumor-specific immune cells in the spleen.

In conclusion, our data demonstrate the ability of systemically administered adenovirus armed with TNF- α and IL-2 to potentiate the therapeutic efficacy of aPD-1 in mouse *in vivo* even in the presence of neutralizing antibodies. Similar trend was observed in human *ex vivo* lung cancer model when an oncolytic virus TILT-123 was used. The mechanism of action appears to involve restoration of NK cell cytotoxicity, reduced immunosuppression, and generation of tumor-specific immunological memory. This approach is currently being translated clinically into an ongoing trial in patients with ICI-refractory NSCLC.

Authors' contributions

- TVK, JC, DCAQ, IAKL, RH, CH, VCC, JMS, SS, OH, AK, EWV, and AH designed experiments.
- TVK, JC, SP, DCAQ, IAKL, SGVK, VA, and EA conducted experiments.
- JR, II, KB, and ES and collected the patient-derived samples;
- TVK, JC, SP, and MIM analyzed the results;
- All the authors contributed to writing and reviewing the manuscript.

Acknowledgments

We thank Minna Oksanen and Susanna Grönberg-Vähä-Koskela for expert experimental and administrative assistance. We also thank Mikko Räsänen, Lotta Ahlfors and Laboratory Animal Center (LAC, University of Helsinki, Helsinki, Finland), Biomedicum Flow Cytometry Unit (University of Helsinki, Helsinki, Finland) and Biomedicum Imaging Unit (University of Helsinki, Helsinki, Finland). Open access funded by the Helsinki University Library (University of Helsinki, Finland).

Disclosure statement

AH is a shareholder in Targovax ASA. AH, JC, JMS, VCC, RH, SS, and DCAQ are employees and shareholders of TILT Biotherapeutics, Ltd. The authors declare no conflicts of interest.

Funding

This study was supported by the Doctoral Program in Clinical Research (University of Helsinki), Jane and Aatos Erkko Foundation, Finnish Cultural Foundation, Ida Montinin Foundation, Orion Foundation,

K. Albin Johansson Foundation, HUCH Research Funds (VTR), Finnish Cancer Organizations, Sigrid Juselius Foundation, Novo Nordisk Foundation, Päivikki and Sakari Sohlberg Foundation, Finnish Red Cross Blood Service, and TILT Biotherapeutics Ltd. This study received funding from the European Union's Horizon 2020 Research and Innovation Programme under Marie Skłodowska-Curie grant agreement No 813453. We thank Albert Ehrnrooth and Karl Fazer for their support. Part of this work was carried out with the support of the HiLIFE Laboratory Animal Center Core Facility, University of Helsinki.

ORCID

Akseli Hemminki  <http://orcid.org/0000-0001-7103-8530>

Availability of data and material

Upon reasonable request.

Ethics statement

All animal experiments described in the paper were approved by the Provincial Government of Southern Finland and the Experimental Animal Committee of the University of Helsinki (license number ESAVI/12559/2021).

Cancer samples were collected from patients undergoing surgical resection at Helsinki University Central Hospital (HUS, Helsinki, Finland). Sample collection was approved by the HUS Ethics Committee (479/17.3.2021; HUS/552/2021), and study permits were obtained (17.05.2021; reference number HUS/259/2021). Written informed consent was obtained from all study participants.

List of abbreviations

NSCLC – non-small cell lung cancer, ICIs – immune checkpoint inhibitors, OVs – oncolytic viruses, aPD-1 – anti-programmed cell death protein 1, IL – interleukin, TNF α – tumor necrosis factor alpha, TME – tumor microenvironment, VP – virus particles, NAB – neutralizing antibodies, IFN γ – interferon gamma, IL, Gzmb – Granzyme B, Perf – Perforin, NK cell – natural killer cell, TAM – tumor-associated macrophages, DCs – dendritic cells, SEM – standard error of the mean.

References

1. Shinohara S, Takahashi Y, Komuro H, Matsui T, Sugita Y, Demachi-Okamura A, Muraoka D, Takahara H, Nakada T, Sakakura N, et al. New evaluation of the tumor immune micro-environment of non-small cell lung cancer and its association with prognosis. *J Immunother Cancer*. 2022 Apr;10(4):e003765. doi:10.1136/jitc-2021-003765.
2. Chang YS, Tu SJ, Chen YC, Liu TY, Lee YT, Yen JC, Fang HY, Chang JG. Mutation profile of non-small cell lung cancer revealed by next generation sequencing. *Respir Res*. 2021 Jan 6;22(1):3. doi:10.1186/s12931-020-01608-5.
3. Mithoowani H, Febbraro M. Non-small-cell lung cancer in 2022: A review for general practitioners in oncology. *Curr Oncol*. 2022 Mar 9;29(3):1828–1839. doi:10.3390/curroncol29030150.
4. Reck M, Ciuleanu TE, Lee JS, Schenker M, Audigier-Valette C, Zurawski B, Linardou H, Otterson GA, Salman P, Nishio M, et al. First-line nivolumab plus ipilimumab versus chemotherapy in advanced NSCLC with 1% or greater tumor PD-L1 expression: Patient-reported outcomes from CheckMate 227 part 1. *J Thorac Oncol*. 2021 Apr;16(4):665–676. doi:10.1016/j.jtho.2020.12.019.
5. Forde PM, Spicer J, Lu S, Provencio M, Mitsudomi T, Awad MM, Felip E, Broderick SR, Brahmer JR, Swanson SJ, et al. Neoadjuvant nivolumab plus chemotherapy in resectable lung cancer. *N Engl*

- J Med. 2022 May 26;386(21):1973–1985. doi:10.1056/NEJMoa2202170.
6. Maione P, Sacco PC, Sgambato A, Casaluca F, Rossi A, Gridelli C. Overcoming resistance to targeted therapies in NSCLC: current approaches and clinical application. *Ther Adv Med Oncol*. 2015 Sep;7(5):263–273. doi:10.1177/1758834015595048.
 7. Jenkins RW, Barbie DA, Flaherty KT. Mechanisms of resistance to immune checkpoint inhibitors. *Br J Cancer*. 2018 Jan;118(1):9–16. doi:10.1038/bjc.2017.434.
 8. Li Z, Feiyue Z, Gaofeng L, Haifeng L. Lung cancer and oncolytic virotherapy—enemy’s enemy. *Transl Oncol*. 2023 Jan;27:101563. doi:10.1016/j.tranon.2022.101563.
 9. Havunen R, Siurala M, Sorsa S, Grönberg-Vähä-Koskela S, Behr M, Tähtinen S, Santos JM, Karell P, Rusanen J, Nettelbeck DM, et al. Oncolytic adenoviruses armed with tumor necrosis factor alpha and interleukin-2 enable successful adoptive cell therapy. *Mol Ther Oncolytics*. 2016 Dec 31;4:77–86. doi:10.1016/j.omto.2016.12.004.
 10. Small EJ, Carducci MA, Burke JM, Rodriguez R, Fong L, van Ummersen L, Yu DC, Aimi J, Ando D, Working P, et al. A phase I trial of intravenous CG7870, a replication-selective, prostate-specific antigen-targeted oncolytic adenovirus, for the treatment of hormone-refractory, metastatic prostate cancer. *Mol Ther*. 2006 Jul;14(1):107–117. doi:10.1016/j.ymthe.2006.02.011.
 11. García M, Moreno R, Gil-Martin M, Cascalló M, de Olza MO, Cuadra C, Piulats JM, Navarro V, Domenech M, Alemany R, et al. A phase I trial of oncolytic adenovirus ICOVIR-5 administered intravenously to cutaneous and uveal melanoma patients. *Hum Gene Ther*. 2019 Mar;30(3):352–364. doi:10.1089/hum.2018.107.
 12. Bottermann M, Foss S, van Tienen LM, Vaysburd M, Cruickshank J, O’Connell K, Clark J, Mayes K, Higginson K, Hirst JC, et al. TRIM21 mediates antibody inhibition of adenovirus-based gene delivery and vaccination. *Proc Natl Acad Sci U S A*. 2018 Oct 9;115(41):10440–10445. doi:10.1073/pnas.1806314115.
 13. Bottermann M, Foss S, Caddy SL, Clift D, van Tienen LM, Vaysburd M, Cruickshank J, O’Connell K, Clark J, Mayes K, et al. Complement C4 prevents viral infection through capsid inactivation. *Cell Host & Microbe*. 2019 Apr 10;25(4):617–629.e7. doi:10.1016/j.chom.2019.02.016.
 14. Zheng M, Huang J, Tong A, Yang H. Oncolytic viruses for cancer therapy: Barriers and Recent Advances. *Mol Ther Oncolytics*. 2019 Nov 2;15:234–247. doi:10.1016/j.omto.2019.10.007.
 15. Shayan S, Arashkia A, Azadmanesh K. Modifying oncolytic virotherapy to overcome the barrier of the hypoxic tumor microenvironment. Where do we stand? *Cancer Cell Int*. 2022 Nov 24;22(1):370. doi:10.1186/s12935-022-02774-w.
 16. Xie R, Bi X, Shang B, Zhou A, Shi H, Shou J. Efficacy and safety of oncolytic viruses in advanced or metastatic cancer: a network meta-analysis. *Virology*. 2021 Jul 31;18(1):158. doi:10.1186/s12985-021-01630-z.
 17. Santos JM, Heiniö C, Cervera-Carrascon V, Quixabeira DCA, Siurala M, Havunen R, Butzow R, Zafar S, de Gruilj T, Lassus H, et al. Oncolytic adenovirus shapes the ovarian tumor microenvironment for potent tumor-infiltrating lymphocyte tumor reactivity. *J Immunother Cancer*. 2020 Jan;8(1):e000188. doi:10.1136/jitc-2019-000188.
 18. Cervera-Carrascon V, Siurala M, Santos JM, Havunen R, Tähtinen S, Karell P, Sorsa S, Kanerva A, Hemminki A. TNF α and IL-2 armed adenoviruses enable complete responses by anti-PD-1 checkpoint blockade. *Oncoimmunology*. 2018 Apr 9;7(5):e1412902. doi:10.1080/2162402X.2017.1412902.
 19. Clubb JHA, Kudling TV, Heiniö C, Basnet S, Pakola S, Cervera Carrascón V, Santos JM, Quixabeira DCA, Havunen R, Sorsa S, et al. Adenovirus encoding tumor necrosis factor alpha and interleukin 2 induces a tertiary lymphoid structure signature in immune checkpoint inhibitor refractory head and neck cancer. *Front Immunol*. 2022 Mar 7;13:794251. doi:10.3389/fimmu.2022.794251.
 20. Heiniö C, Clubb J, Kudling T, Quixabeira D, Cervera-Carrascon V, Havunen R, Grönberg-Vähä-Koskela S, Santos JM, Tapper J, Kanerva A, et al. Effective combination immunotherapy with oncolytic adenovirus and anti-PD-1 for treatment of human and murine ovarian cancers. *Diseases*. 2022 Aug 8;10(3):52. doi:10.3390/diseases10030052.
 21. Havunen R, Santos JM, Sorsa S, Rantapero T, Lumen D, Siurala M, Airaksinen AJ, Cervera-Carrascon V, Tähtinen S, Kanerva A, et al. Abscopal effect in non-injected tumors achieved with cytokine-armed oncolytic adenovirus. *Mol Ther Oncolytics*. 2018 Nov 6;11:109–121. doi:10.1016/j.omto.2018.10.005.
 22. Siurala M, Havunen R, Saha D, Lumen D, Airaksinen AJ, Tähtinen S, Cervera-Carrascon V, Bramante S, Parviainen S, Vähä-Koskela M, et al. Adenoviral delivery of tumor necrosis factor- α and interleukin-2 enables successful adoptive cell therapy of immunosuppressive melanoma. *Mol Ther*. 2016 Aug;24(8):1435–1443. doi:10.1038/mt.2016.137.
 23. Kanerva A, Mikheeva GV, Krasnykh V, Coolidge CJ, Lam JT, Mahareshti PJ, Barker SD, Straughn M, Barnes MN, Alvarez RD, et al. Targeting adenovirus to the serotype 3 receptor increases gene transfer efficiency to ovarian cancer cells. *Clin Cancer Res*. 2002 Jan;8(1):275–280.
 24. Coudray-Meunier C, Fraisse A, Martin-Latil S, Guillier L, Perelle S. Discrimination of infectious hepatitis A virus and rotavirus by combining dyes and surfactants with RT-Qpcr. *BMC Microbiol*. 2013 Oct 1;13:216. doi:10.1186/1471-2180-13-216.
 25. Leifels M, Cheng D, Sozzi E, Shoults DC, Wuertz S, Mongkolsuk S, Sirikanchana K. Capsid integrity quantitative PCR to determine virus infectivity in environmental and food applications – a systematic review. *Water Research X*. 2021;11:100080. doi:10.1016/j.wroa.2020.100080.
 26. Kohanbash G, McKaveney K, Sakaki M, Ueda R, Mintz AH, Amankulor N, Fujita M, Ohlfest JR, Okada H. GM-CSF promotes the immunosuppressive activity of glioma-infiltrating myeloid cells through interleukin-4 receptor- α . *Cancer Res*. 2013 Nov 1;73(21):6413–6423. doi:10.1158/0008-5472.CAN-12-4124.
 27. Hong IS. Stimulatory versus suppressive effects of GM-CSF on tumor progression in multiple cancer types. *Experimental & Molecular Medicine*. 2016 Jul 1;48(7):e242. doi:10.1038/emm.2016.64.
 28. Tähtinen S, Kaikkonen S, Merisalo-Soikkeli M, Grönberg-Vähä-Koskela S, Kanerva A, Parviainen S, Vähä-Koskela M, Hemminki A, Shiku H. Favorable alteration of tumor microenvironment by immunomodulatory cytokines for efficient T-cell therapy in solid tumors. *PLoS One*. 2015 Jun 24;10(6):e0131242. doi:10.1371/journal.pone.0131242.
 29. Baumeister SH, Freeman GJ, Dranoff G, Sharpe AH. Coinhibitory Pathways in Immunotherapy for Cancer. *Annu Rev Immunol*. 2016;34(1):539–573. doi:10.1146/annurev-immunol-032414-112049.
 30. Fushimi T, Kojima A, Moore MA, Crystal RG. Macrophage inflammatory protein 3 α transgene attracts dendritic cells to established murine tumors and suppresses tumor growth. *J Clin Invest*. 2000 May;105(10):1383–1393. doi:10.1172/JCI7548.
 31. Kikuchi T, Crystal RG. Anti-tumor immunity induced by in vivo adenovirus vector-mediated expression of CD40 ligand in tumor cells. *Hum Gene Ther*. 1999 May 20;10(8):1375–1387. doi:10.1089/10430349950018049.
 32. Hollern DP, Xu N, Thennavan A, Glodowski C, Garcia-Recio S, Mott KR, He X, Garay JP, Carey-Ewend K, Marron D, et al. B cells and T follicular helper cells mediate response to checkpoint inhibitors in high mutation burden mouse models of breast cancer. *Cell*. 2019 Nov 14;179(5):1191–1206.e21. doi:10.1016/j.cell.2019.10.028.
 33. Petitprez F, de Reyniès A, Keung EZ, Chen TW, Sun CM, Calderaro J, Jeng YM, Hsiao LP, Lacroix L, Bougouïn A, et al. B cells are associated with survival and immunotherapy response in sarcoma. *Nature*. 2020 Jan;577(7791):556–560. doi:10.1038/s41586-019-1906-8.
 34. Xu Z, Tian J, Smith JS, Byrnes AP. Clearance of adenovirus by Kupffer cells is mediated by scavenger receptors, natural antibodies, and complement. *J Virol*. 2008 Dec;82(23):11705–11713. doi:10.1128/JVI.01320-08.
 35. Zafar S, Quixabeira DCA, Kudling TV, Cervera-Carrascon V, Santos JM, Grönberg-Vähä-Koskela S, Zhao F, Aronen P,

- Heiniö C, Havunen R, et al. Ad5/3 is able to avoid neutralization by binding to erythrocytes and lymphocytes. *Cancer Gene Ther.* 2021 May;28(5):442–454. doi:10.1038/s41417-020-00226-z.
36. Hamilton G, Plangger A. The impact of NK cell-based therapeutics for the treatment of lung cancer for biologics: Targets and therapy. *Biologics.* 2021 Jul 7;15:265–277. doi:10.2147/BTT.S290305.
37. Casanova-Acebes M, Dalla E, Leader AM, LeBerichel J, Nikolic J, Morales BM, Brown M, Chang C, Troncoso L, Chen ST, et al. Tissue-resident macrophages provide a pro-tumorigenic niche to early NSCLC cells. *Nature.* 2021 Jul;595(7868):578–584. doi:10.1038/s41586-021-03651-8.
38. Zhang J, Rousseaux N, Walzer T. Eomes and T-bet, a dynamic duo regulating NK cell differentiation. *Bioessays.* 2022 Mar;44(3):e2100281. doi:10.1002/bies.202100281.
39. Gill S, Vasey AE, De Souza A, Baker J, Smith AT, Kohrt HE, Florek M, Gibbs KD Jr, Tate K, Ritchie DS, et al. Rapid development of exhaustion and down-regulation of eomesodermin limit the anti-tumor activity of adoptively transferred murine natural killer cells. *Blood.* 2012 Jun 14;119(24):5758–5768. doi:10.1182/blood-2012-03-415364.
40. Huang C, Bi J. Expression regulation and function of T-Bet in NK cells. *Front Immunol.* 2021 Oct 5;12:761920. doi:10.3389/fimmu.2021.761920.
41. Niu C, Li M, Zhu S, Chen Y, Zhou L, Xu D, Xu J, Li Z, Li W, Cui J. PD-1-positive natural killer cells have a weaker anti-tumor function than that of PD-1-negative natural killer cells in lung cancer. *Int J Med Sci.* 2020 Jul 19;17(13):1964–1973. doi:10.7150/ijms.47701.
42. Qiao DR, Cheng JY, Yan WQ, Li HJ. PD-L1/PD-1 blockade enhanced the cytotoxicity of natural killer cell on the non-small cell lung cancer (NSCLC) by granzyme B secretion. *Clin Transl Oncol.* 2023 Mar 1;25(8):2373–2383. doi:10.1007/s12094-023-03120-w.
43. Zalfa C, Paust S. Natural killer cell interactions with myeloid derived suppressor cells in the tumor microenvironment and implications for cancer immunotherapy. *Front Immunol.* 2021 May 5;12:633205. doi:10.3389/fimmu.2021.633205.
44. Wang JB, Huang X, Li FR. Impaired dendritic cell functions in lung cancer: a review of recent advances and future perspectives. *Cancer Commun (Lond).* 2019 Jul 15;39(1):43. doi:10.1186/s40880-019-0387-3.
45. Russo E, Laffranchi M, Tomaipitina L, Del Prete A, Santoni A, Sozzani S, Bernardini G. NK cell anti-tumor surveillance in a myeloid cell-shaped environment. *Front Immunol.* 2021 Dec 17;12:787116. doi:10.3389/fimmu.2021.787116.
46. Paschall AV, Zhang R, Qi CF, Bardhan K, Peng L, Lu G, Yang J, Merad M, McGaha T, Zhou G, et al. IFN regulatory factor 8 represses GM-CSF expression in T cells to affect myeloid cell lineage differentiation. *The Journal Of Immunology query.* 2015 Mar 1;194(5):2369–2379. doi:10.4049/jimmunol.1402412.
47. Li HY, McSharry M, Bullock B, Nguyen TT, Kwak J, Poczobutt JM, Sippel TR, Heasley LE, Weiser-Evans MC, Clambey ET, et al. The tumor microenvironment regulates sensitivity of murine lung tumors to PD-1/PD-L1 antibody blockade. *Cancer Immunol Res.* 2017 Sep;5(9):767–777. doi:10.1158/2326-6066.CIR-16-0365.
48. Li S, Simoni Y, Zhuang S, Gabel A, Ma S, Chee J, Islas L, Cessna A, Creaney J, Bradley RK, et al. Characterization of neoantigen-specific T cells in cancer resistant to immune checkpoint therapies. *Proc Natl Acad Sci U S A.* 2021 Jul 27;118(30):e2025570118. doi:10.1073/pnas.2025570118.